Syst. Biol. 49(4):740–753, 2000

Use of Two-Block Partial Least-Squares to Study Covariation in Shape

F. JAMES ROHLF[1] AND MARCO CORTI[2]

[1]*Department of Ecology and Evolution, State University of New York, Stony Brook, New York 11794-5245, USA; E-mail: rohlf@life.bio.sunysb.edu*

[2]*Dipartimento di Biologia Animale e dell'Uomo, Universita'di Roma "La Sapienza," via Borelli 50, 00161 Roma, Italy; E-mail: corti@axrma.uniroma1.it*

Abstract.—The relatively new two-block partial least-squares method for analyzing the covariance between two sets of variables is described and contrasted with the well-known method of canonical correlation analysis. Their statistical properties, types of answers, and visualization techniques are discussed. Examples are given to show its usefulness in comparing two sets of variables—especially when one or both of the sets of variables are shape variables from a geometric morphometric study. [Canonical correlation; covariance; morphometrics; *Mus musculus domesticus*; partial least squares; *Plethodon*; visualization.]

In this article we describe the application to morphometrics of two-block partial least-squares (2B-PLS) analysis (Sampson et al., 1989; Streissguth et al., 1993), a relatively new statistical method that can be used to explore patterns of covariation between two sets of variables. This method differs from regression analysis in that the two sets of variables are treated symmetrically rather than one set of variables (independent variables) being used to predict variation in the other set of variables (dependent variables). Although the method has similarities to the well-known method of canonical correlation analysis (Jackson, 1991), it is distinct and is used to answer a somewhat different question. The 2B-PLS method is just one example of the partial least-squares approach that has been used more often in the social sciences (see Bookstein, 1982, 1986; Jöreskog and Wold, 1982). References to partial least-squares analyses in a nonmorphometric context include Bookstein et al. (1996) and McIntosh et al. (1996).

We compare the 2B-PLS method with canonical correlation analysis (CCA) because that technique is used to answer similar questions. We also show how 2B-PLS can be applied in morphometrics where one or both sets of variables are shape variables such as landmark coordinates of Procrustes aligned specimens or partial warp scores (Bookstein, 1991; Rohlf, 1993). This kind of analysis is expected to be useful for many types of exploratory studies in systematics. It also can be used for confirmatory studies when one has hypotheses about the expected pattern of covariances between two sets of variables (see Streissguth et al., 1993, for examples). Rohlf and Marcus (1993) have given a general introductory overview to the field of geometric morphometrics. Bookstein (1991) gave a comprehensive account, and Small (1996) covered mathematical details. Dryden and Mardia (1998) covered many aspects of shape statistics, Rohlf (1999) discussed the relationships between generalized Procrustes aligned coordinates and partial warp scores, and Marcus et al. (1996) provided both introductory material and examples of applications to many fields of biology and medicine. The fundamental advances of geometric morphometrics over traditional approaches are in the development of powerful statistical methods designed for analysis of shape data rather than the use of standard multivariate methods on ad hoc collections of distances, angles, and ratios.

2B-PLS ANALYSIS

The 2B-PLS method is used to explore the pattern of covariation between two sets of variables. If one partitions an $n \times p$ data matrix, $\mathbf{Y}$, by columns into $\mathbf{Y}_1$ and $\mathbf{Y}_2$ (with p_1 and p_2 columns, respectively), then 2B-PLS constructs pairs of variables that are linear combinations of the variables within each of the two sets. The linear combinations are constructed so that the new variables account for as much as possible of the covariation between the two original sets of variables. These new variables are expected to be useful for describing whatever patterns of covariation exist between the two sets of original variables.

TABLE 1. Correlations among six (relative) morphological measurements of chickens. Data from Dunn (1922) as corrected by Marcus (1990).

	Skull length	Skull breadth	Fibula	Tibia	Humerus	Ulna
Skull length	1	0.584	0.615	0.610	0.570	0.600
Skull breadth	0.584	1	0.576	0.530	0.526	0.555
Fibula	0.615	0.576	1	0.940	0.875	0.878
Tibia	0.610	0.530	0.940	1	0.877	0.886
Humerus	0.570	0.526	0.875	0.877	1	0.924
Ulna	0.600	0.555	0.878	0.886	0.924	1

We shall use a well-known data set to help us describe the method, measurements of lengths and widths of skull and limb bones from chickens (Dunn, 1922, as corrected by Marcus, 1990). The matrix of correlations, **R**, is given in Table 1. The raw data are not available, but most of the 2B-PLS computations can be performed by using only a correlation matrix. However, the lack of raw data prevents us from making important diagnostic plots. Examples of these plots are given below for other data sets. Table 1 also indicates partitioning of the correlation matrix into sets consisting of two skull measurements and four limb bone measurements. Symbolically, we can represent this partitioning as

$$\mathbf{R} = \begin{pmatrix} \mathbf{R}_{11} & \mathbf{R}_{12} \\ \mathbf{R}_{21} & \mathbf{R}_{22} \end{pmatrix},$$

where $\mathbf{R}_{21} = \mathbf{R}_{12}^t$ (matrix transpose is indicated by a superscript t). The 2B-PLS method decomposes the $\mathbf{R}_{12}$ matrix into the product $\mathbf{F}_1\mathbf{D}\mathbf{F}_2^t$ by the use of a singular value decomposition (Eckart and Young, 1936; Jackson, 1991). The matrix **D** is diagonal and contains the singular values, λ_i. The values in each column of $\mathbf{F}_1$ are the weights for the linear combinations for the variables in the first set, and the values in the corresponding columns of $\mathbf{F}_2$ give those for the variables in the second set. The number of rows corresponds to the number of variables, p_1 and p_2, in each set. The number of columns (dimensions) is p_1 or p_2, whichever is less. The first k columns of $\mathbf{F}_1$ and $\mathbf{F}_2$ can be interpreted as yielding the best least-squares approximation of $\mathbf{R}_{21}$, the matrix of correlations between the two sets of variables. The adequacy of the approximation can be measured by $\sum_i^k(\lambda_i^2/\sum\lambda_i^2$. The denominator, $\sum\lambda_i^2$, is also equal to the sum of the squared elements in the $\mathbf{R}_{21}$ matrix and is a measure of the total amount of covariance between the two sets of variables. Given that the maximum possible value of $\sum\lambda_i^2$ is $p_1 \times p_2$ (the value that would be obtained if all the correlations were equal to 1), $\sum\lambda_i^2/p_1p_2$ gives a measure of the overall squared covariance between the two sets of variables. Streissguth et al. (1993) and Bookstein et al. (1996) provide additional interpretations of 2B-PLS.

The $\mathbf{F}_1$ and $\mathbf{F}_2$ matrices and the singular values are given in Table 2. The solution is essentially one-dimensional because the first pair of vectors accounts for $1.6191^2/(1.6191^2 + 0.0184^2) = 0.9987$ of the total covariation between the two sets of variables. However, both dimensions together represent just $(1.6191^2 + 0.0184^2)/(2 \times 4) = 0.3277$ of the total possible squared covariance. The first latent variable is essentially just an equally weighted sum of variables in set 1 and set 2 because the coefficients (saliences) in the first columns of $\mathbf{F}_1$ and $\mathbf{F}_2$ are quite similar. One cannot directly compare the magnitudes of the elements of the $\mathbf{F}_1$ and $\mathbf{F}_2$ matrices because they are scaled so that the squared values sum to 1. For comparing or plotting different columns within the $\mathbf{F}_1$ and $\mathbf{F}_2$ matrices, they should first be multiplied by their corresponding singular values.

If the original data were available, one could compute matrices giving the scores

TABLE 2. Results of partial least-squares analysis of the correlation matrix in Table 1.

		Dimensions	
Matrix	Variable	1	2
$\mathbf{F}_1$	Skull length	0.737	0.676
	Skull breadth	0.676	−0.737
$\mathbf{F}_2$	Fibula	0.520	−0.485
	Tibia	0.495	0.841
	Humerus	0.479	−0.136
	Ulna	0.505	−0.196
Singular value		1.619	0.018
Correlation		0.670	0.107

(estimated measurements) of the new variables for the specimens. These would be computed as $\mathbf{Z}_1 = \mathbf{Y}_1\mathbf{F}_1$ and $\mathbf{Z}_2 = \mathbf{Y}_2\mathbf{F}_2$, where $\mathbf{Y}_1$ and $\mathbf{Y}_2$ have been standardized because the matrix $\mathbf{R}_{12}$ contains correlations. One could then construct various plots and compute the correlations among these new variables. It is also possible to compute these correlations (including the correlations between corresponding variables from each set) indirectly as $\mathbf{R}_{\mathbf{F}_1\mathbf{F}_2} = \mathbf{S}^{-1/2}\mathbf{F}^t\mathbf{R}\mathbf{F}\mathbf{S}^{-1/2}$, where

$$\mathbf{F} = \begin{bmatrix} \mathbf{F}_1 & \mathbf{0} \\ \mathbf{0} & \mathbf{F}_2 \end{bmatrix},$$

is a block diagram matrix and $\mathbf{S} = \text{diag}(\mathbf{F}^t\mathbf{R}\mathbf{F})$. The results are shown in Table 3. The off-diagonal block of $\mathbf{R}_{\mathbf{F}_1\mathbf{F}_2}$ is of particular interest, because it contains the correlations between the paired variables for each set. In computing these, one can take advantage of the fact that. $\mathbf{F}_1^t\mathbf{R}_{12}\mathbf{F}_2 = \mathbf{D}$. In our example, the correlations are 0.670 and 0.107. The first is larger than any of the observed correlations but not quite as large as the first canonical correlation (0.684). Note that the PLS vectors are correlated within each set of variables (unlike the analogous vectors in a CCA).

Computation of the correlations between all of the variables and the columns of $\mathbf{Z}_1$ and $\mathbf{Z}_2$ is also interesting. These can be computed indirectly as $\mathbf{S}^{-1/2}\mathbf{F}^t\mathbf{R}$. As one would expect for these data, the vectors are highly correlated both with the variables within their sets and with the variables of the other set. The correlations for the second pair of vectors are much lower and are of little interest because this dimension accounts for so little of the between-set covariation.

Residuals of the correlation matrix, $\mathbf{R}_{12}$, can be computed by using the expression $\mathbf{F}\mathbf{C}\mathbf{R}_{\mathbf{F}_1\mathbf{F}_2}\mathbf{C}\mathbf{F}^t$, where $\mathbf{C}$ is a diagonal matrix with 1's and 0's on the diagonal to indicate which dimensions are included or excluded, respectively, from the model. The residuals are computed this way to take into account the within-set correlations among the vectors. For these data, the residuals are quite small after removing the effects of the first dimension. After the effects of both dimensions have been removed, the $\mathbf{R}_{11}$ and $\mathbf{R}_{12}$ residuals are equal to zero. The $\mathbf{R}_{22}$ residuals are not expected to equal zero because there are more variables in set 2 than in set 1. To account for all of the correlation among variables in set 2, one would have to introduce dimensions that describe variation within the second set.

TABLE 3. Results of partial least-squares analysis of correlation matrix in Table 1. Correlations within and among columns of $\mathbf{F}_1$ and $\mathbf{F}_2$ as identified in Table 2.

		$\mathbf{F}_1$		$\mathbf{F}_2$	
		1	2	1	2
$\mathbf{F}_1$	1	1.000	−0.062	0.670	0.000
	2	−0.062	1.000	0.000	0.106
$\mathbf{F}_2$	1	0.670	0.000	1.000	0.100
	2	0.000	0.106	0.100	1.000

CANONICAL CORRELATION ANALYSIS

It is useful to compare these results with those obtained by the more familiar CCA. Jackson (1991) and Manly (1994) gave good introductions to this classic technique. If there is only a single variable in one set, then the CCA reduces to multiple regression analysis with the coefficients for the linear combination of the variables becoming standardized partial regression coefficients. Thus, CCA can be viewed as a generalization of multiple regression. The purpose of CCA is to find canonical variables (linear combinations of the variables) in each set such that the correlation between the corresponding canonical variables in each set is as large as possible. It is possible for the linear combinations to be quite different from those obtained by 2B-PLS because different criteria are being optimized. Moreover, the linear combinations with the highest correlation between the two sets need not explain much of the covariance between the two sets of variables.

The computational steps are more complex than those in 2B-PLS. In addition to $\mathbf{R}_{12}$, CCA also uses $\mathbf{R}_{11}$ and $\mathbf{R}_{22}$, the correlations among the variables within each set. The matrix of vectors, $\mathbf{F}_1$, for the first set is $\mathbf{R}_{11}^{-1/2}$ times the eigenvectors of $\mathbf{R}_{11}^{-1/2}\mathbf{R}_{12}\mathbf{R}_{22}^{-1}\mathbf{R}_{21}\mathbf{R}_{11}^{-1/2}$, scaled so that $\text{diag}(\mathbf{F}_1^t\mathbf{R}_{11}\mathbf{F}_1) = \mathbf{I}$, where $\mathbf{I}$ is the identity matrix. By interchanging the 1's and 2's in these equations one obtains the corresponding computations for $\mathbf{F}_2$. The eigenvalues are the same in both cases and are equal to the squared canonical correlations. As in 2B-PLS, the maximum number of dimensions is $\min(p_1, p_2)$. The eigenvalues can be used to express the concentration of the

TABLE 4. Results of a canonical correlation analysis of the correlation matrix in Table 1: matrices $\mathbf{F}_1$ and $\mathbf{F}_2$.

Matrix	Variable	Dimensions 1	2
$\mathbf{F}_1$	Skull length	0.630	−1.059
	Skull breadth	0.492	1.129
$\mathbf{F}_2$	Fibula	0.733	2.459
	Tibia	−0.096	−3.132
	Humerus	−0.118	0.078
	Ulna	0.502	0.468
Eigenvalue		0.468	0.012
Canonical correlation		0.684	0.112

covariation into each dimension (from a total equal to the minimum of p_1 and p_2).

The $\mathbf{F}_1$ and $\mathbf{F}_2$ matrices and the eigenvalues are given in Table 4. The solution is essentially one-dimensional because the first eigenvalue is much larger than the second. The correlation between the first pair of latent variables is 0.684, slightly more than the equivalent correlation found by using 2B-PLS. This first pair of canonical variables accounts for $0.468/2 = 0.234$ of the total possible covariation between the two sets of variables, somewhat less than that found by 2B-PLS.

The first column of $\mathbf{F}_1$ corresponds to the sum of the two variables (again with a greater weight given to the first variable). The first column of $\mathbf{F}_2$ is, curiously, essentially the sum of the first and last variables (with a greater weight to the first variable). This does not seem to make much sense biologically. However, computing the correlations between each variable and the columns of $\mathbf{Z}_1$ and $\mathbf{Z}_2$ (computed indirectly as $\mathbf{S}^{-1/2}\mathbf{F}^t\mathbf{R}$) reveals that all the variables have large positive correlations with the first column of both $\mathbf{Z}_1$ and $\mathbf{Z}_2$. Despite the coefficients in the first column of $\mathbf{F}_1$ and $\mathbf{F}_2$, the first dimension essentially just measures overall size within each set. The coefficients of $\mathbf{F}_1$ and $\mathbf{F}_2$ must therefore be interpreted as one does partial regression coefficients; they indicate the contribution of a variable when the effects of other variables are held constant. Thus if one of a pair of highly correlated variables has a large coefficient, the second will tend not to, because it will have relatively little to contribute once the effects of the first variable have been held constant. One of the attractions of 2B-PLS is that its coefficients do not have this property and thus can be interpreted more directly. Another difference is that a CCA cannot be performed if the sample size is equal to or less than the number of variables in either set.

TABLE 5. Results of a canonical correlation analysis of the correlation matrix in Table 1: correlations within and among columns of $\mathbf{F}_1$ and $\mathbf{F}_2$.

		$\mathbf{F}_1$ 1	$\mathbf{F}_1$ 2	$\mathbf{F}_2$ 1	$\mathbf{F}_2$ 2
$\mathbf{F}_1$	1	1.000	0.000	0.684	0.000
	2	0.000	1.000	0.000	0.112
$\mathbf{F}_2$	1	0.670	0.000	1.000	0.000
	2	0.000	0.112	0.000	1.000

In analogy to the method used in 2B-PLS, the correlations between pairs of variables can be computed indirectly as $\mathbf{S}^{-1/2}\mathbf{F}^t\mathbf{R}\mathbf{F}\mathbf{S}^{-1/2}$, where $\mathbf{S} = \text{diag}(\mathbf{F}^t\mathbf{R}\mathbf{F})$ and

$$\mathbf{F} = \begin{bmatrix} \mathbf{F}_1 & \mathbf{0} \\ \mathbf{0} & \mathbf{F}_2 \end{bmatrix}.$$

The results are shown in Table 5. Note that the latent variables are not correlated within each set (in contrast to Table 3), a consequence of the additional constraints in a CCA. Because the columns of $\mathbf{F}$ are orthogonal, the residuals can be computed as $\mathbf{R} - \mathbf{F}\mathbf{F}^t$. The entire residual matrix will be essentially zero if both dimensions are used.

GENERALIZATION TO STUDY COVARIATION WITH SHAPE

The 2B-PLS method can also be used to analyze the covariation with shape by simply using shape variables as one of the sets of variables. Although shape variables can be constructed in many ways (e.g., ad hoc collections of interlandmark distances, ratios, and angles), the methods of geometric morphometrics offer many advantages and will be used below.

The most direct source of shape variables is to use the x, y (or x, y, z for three-dimensional data) coordinates of the locations of p morphological landmarks after they have been aligned to their average shape by use of a generalized least-squares Procrustes analysis (GLS; Rohlf and Slice, 1990). This alignment removes the effects of variation in location, orientation, and scale from the coordinates. The average configuration of landmarks is often called the consensus or the reference configuration. Although these effects are usually small, the aligned coordinates should be projected onto the

linear tangent space that is orthogonal to the average shape (Rohlf, 1999). The matrix of projections into tangent space can be computed as

$$\mathbf{X}' = \mathbf{X}\left(\mathbf{I}_{2p} - \mathbf{X}_c^t\mathbf{X}_c\right),$$

where $\mathbf{X}$ is the $n \times 2p$ matrix of n aligned specimens (each specimen scaled to unit centroid size and with coordinates in a single row with $2p$ elements), $\mathbf{I}_{2p}$ is a $2p \times 2p$ identity matrix, and $\mathbf{X}_c$ is the reference configuration (also scaled to unit centroid size and stored as a row vector with $2p$ elements). This step projects the specimens into what Kent (1994) called Kendall tangent space (see Rohlf, 1999, for further details).

The new coordinates provide $2p$ shape variables ($3p$ for three-dimensional data). These variables are redundant (their covariance matrix will be singular) because only $2p - 4$ (or $3p - 7$ for three-dimensional data) variables are required to account for any possible shape variation among p landmarks. A mathematically equivalent approach (see Rohlf, 1999) is to use partial warp scores (including the uniform component). This choice is convenient because the variables are not redundant. This redundancy does not interfere with the computations in a 2B-PLS analysis, and identical correlations and proportions of covariance explained are obtained with either type of shape variables. CCA, on the other hand, cannot be applied to redundant variables. The linear combinations of shape variables produced by the 2B-PLS analysis can be directly expressed as deformations by using thin-plate splines. These correspond to the same shape differences that would be obtained if using the Procrustes coordinates as the shape variables. The use of partial warps also makes it possible to emphasize shape differences at different spatial scales—a property that might be useful in some applications. Expressing the shape changes as a deformation by using the thin-plate spline has the advantage of integrating the landmark displacements at all landmarks. This is helpful because it is sometimes difficult to appreciate the overall shape change by looking at apparent displacements at individual landmarks. Bookstein (1989, 1991) and Rohlf (1993) give the details of the computation of partial warps. The next section discusses the generalization to analyses where both sets of variables are shape variables.

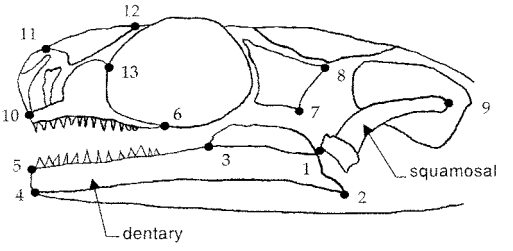

FIGURE 1. Positions of 13 landmarks from a left lateral view of a *Plethodon* skull. The dentary and squamosal are identified. Diagram based on Adams (1999).

The following example was taken from a larger study (Adams, 1999) investigating the relationships between trophic morphology and the types of prey consumed in *Plethodon* salamanders. This data set comprized 38 *P. hoffmani* and 31 *P. cinereus* specimens collected from a single locality in Pennsylvania. For each specimen, the locations of 13 landmarks on the skull and jaw were digitized from a lateral view in which the jaw was kept open at a fixed angle to standardize the jaw position (Fig. 1). In addition, the stomach contents of each specimen were recorded as the numbers of prey in each of 16 categories. The categories were ordered with the frequency of the smallest prey (Acarina) as variable 1 and that of the largest prey (Chilopoda) as variable 16. Because the counts were expected to be Poisson rather than normally distributed, they were square-root transformed.

The first computational steps are to obtain a consensus configuration using GLS and rotate it to its principal axes to simplify the computation of the uniform shape component (Bookstein, 1996). The specimens are then aligned to the consensus configuration. Figure 2 shows the consensus configuration with the 69 specimens superimposed. The scatter represents the variation in shape that we will attempt to correlate with variation in stomach contents.

If partial warps are to be used as shape variables, then for two-dimentional data the $n \times (2p - 4)$ matrix of partial warp scores can be computed as $\mathbf{W} = \mathbf{VP}$, where $\mathbf{V}$ is a matrix whose n rows of kp elements give the differences, $\mathbf{X}_i - \mathbf{X}_c$, between each aligned specimen and the reference. The matrix

$$\mathbf{P} = \left(\begin{array}{c|c} \mathbf{E}\boldsymbol{\Lambda}^{-\alpha/2} & \mathbf{0} \\ \hline \mathbf{0} & \mathbf{E}\boldsymbol{\Lambda}^{-\alpha/2} \end{array}\middle|\, \mathbf{U}\right)$$

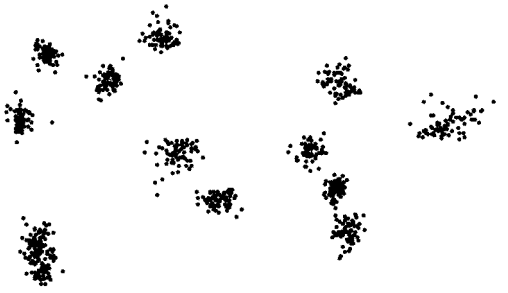

FIGURE 2. GLS Procrustes superimposition of the landmarks from a lateral view of a *Plethodon* skull oriented as in Figure 1.

has orthogonal columns and both projects the specimens into the tangent space and rotates them to the partial warp axes. In this equation, **E** is the $p \times (p-3)$ matrix of principal warps (normalized eigenvectors of the bending energy matrix; Bookstein, 1991), $\mathbf{\Lambda}$ is the diagonal matrix of eigenvalues (λ_i) of the bending energy matrix, and **U** is a matrix that spans the part of tangent space corresponding to uniform shape changes. $\alpha > 0$ results in an emphasis on larger-scale shape features, $\alpha < 0$ gives greater emphasis to smaller-scale features (Rohlf, 1993). $\alpha = 0$ gives equal weight to variation at all spatial scales—which seems appropriate in most systematic studies. Bookstein (1997) shows examples of the use of other values for α. The uniform component should not be included unless $\alpha = 0$.

The scores for the uniform component can be computed as **VU**. For two-dimensional data Bookstein's (1996) linearized Procrustes estimate can be expressed as

$$\mathbf{U} = \begin{pmatrix} \sqrt{\frac{\alpha}{\gamma}}y_1 & -\sqrt{\frac{\gamma}{\alpha}}x_1 \\ \sqrt{\frac{\alpha}{\gamma}}y_2 & -\sqrt{\frac{\gamma}{\alpha}}x_2 \\ \vdots & \vdots \\ \sqrt{\frac{\alpha}{\gamma}}y_p & -\sqrt{\frac{\gamma}{\alpha}}x_p \\ \sqrt{\frac{\gamma}{\alpha}}x_1 & \sqrt{\frac{\alpha}{\gamma}}y_1 \\ \vdots & \vdots \\ \sqrt{\frac{\gamma}{\alpha}}x_p & \sqrt{\frac{\alpha}{\gamma}}y_p \end{pmatrix},$$

where x and y are landmark coordinates in the rotated reference, $\alpha = \sum x_i^2$ and $\gamma = \sum y_i^2$ (note that the α in this formula is not related to the α parameter used to weight the partial warps). This formula does not yield the same values as given by Rohlf (1996). This procedure can be generalized for three-dimensional data but explicit equations have not yet been developed.

Because the partial warps are all in the same units, it is desirable to perform the 2B-PLS analysis by using covariances rather than standardizing them or using correlations. Using covariances gives more weight to those aspects of shape variation with more variability. Using unstandardized partial warps also makes it possible to use the α parameter to weight the partial warps according to their spatial scale (standardization would remove the effects of such weights). However, the matrix of variables being analyzed for their relationships with shape should be standardized unless the variables are in the same units. In our example, the trophic variables are all square roots of counts and thus should not be standardized. The $\mathbf{R}_{12}$ matrix will then contain covariances between the unstandardized trophic variables and the unstandardized shape variables.

The $\mathbf{R}_{12}$ matrix is then factored into a product $\mathbf{F}_1\mathbf{D}\mathbf{F}_2^t$ as before. The matrix $\mathbf{F}_1$ gives the vectors for the variables and $\mathbf{F}_2$ gives the corresponding vectors for the shape variables (partial warps in our case). **D** is a diagonal matrix of singular values. For two-dimensional data, p_2 is either $2p$ (for aligned coordinates) or $2p-4$ (for partial warps that include the uniform component). The maximum number of nonzero singular values is the minimum of p_1, p_2, and $n-1$. For our example this is 16, given that the trophic variables are fewer than the shape variables or the specimens.

Table 6 gives the singular values and the correlations for the first three paired latent variables. These dimensions explain 92.8%, 2.8%, and 1.8% of the total squared covariance (0.00323) between the two sets of variables. To assess whether more of the covariation is more concentrated into the first few dimensions than would be expected by chance, one can use a permutation test, repeating the calculations described above but randomly permuting the ordering of the specimens for either the variables or the shape variables. Doing this 999 times (a random sample with

TABLE 6. Results of a partial least-squares analysis of the covariation between the square roots of the numbers of different kinds of prey items found in the stomach and the partial warps for the *Plethodon* data.

	Dimensions		
Variable	1	2	3
Acarina	0.028	0.039	0.037
Eggs	−0.004	0.139	−0.171
Isoptera	0.020	−0.190	0.071
Collembola	0.015	−0.118	0.141
Chelonethida	0.026	0.004	0.042
Hymenoptera	−0.578	0.005	0.656
Gastropoda	0.106	0.134	0.278
Larvae	−0.073	0.409	0.226
Coleoptera	0.679	−0.342	0.472
Diptera	−0.291	−0.185	0.169
Araneida	0.078	0.130	0.078
Isopoda	0.260	0.754	0.152
Orthoptera	−0.051	0.061	−0.221
Diplopoda	0.042	0.009	−0.054
Oligochaeta	0.153	−0.001	0.224
Chilopoda	−0.017	0.057	0.025
Singular values	0.0547	0.0096	0.0076
Correlations	0.725	0.557	0.442

replacement out of the 69! possible permutations) and the observed values added to make 1,000 samples, we found that none of the sampled values for the first dimension, were equal to or larger than the observed value. For the other dimensions, all of the random samples yielded greater squared covariances than were found in the observed data. Because the first dimension explained most of the variance and the other dimensions were not statistically significant, one can expect to interpret only the first dimension in this example.

Given that the raw data for this investigation are available, we could compute matrices of scores, $\mathbf{Z}_1$ and $\mathbf{Z}_2$, by using the equations given in the previous section. A scatterplot of the first columns of $\mathbf{Z}_1$ and $\mathbf{Z}_2$ is shown in Figure 3. The correlations between $\mathbf{Z}_1$ and $\mathbf{Z}_2$ for the first three dimensions are 0.725, 0.557, and 0.442, respectively. We could also assess these correlations by a permutation test. We found that none of the random permutations yielded correlations that equaled or exceeded the observed correlation for the first dimension. For the second and third dimensions, the observed correlations were exceeded in 1.0% and 39.0% of the samples, respectively. Although the correlation for the second dimension is statistically different from zero, attempting to interpret the second dimension does not seem worthwhile, because it accounts for so little of the covariance between the trophic and shape variables.

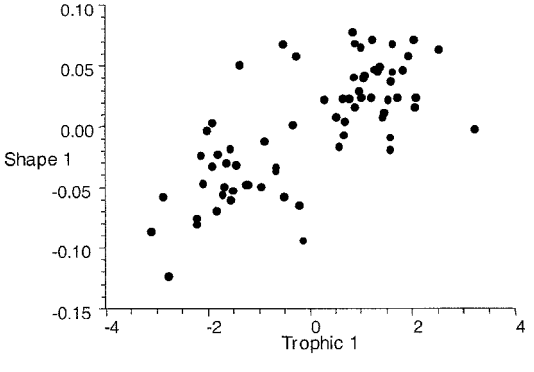

FIGURE 3. Plot of the first column of $\mathbf{Z}_2$ (shape variables) against the first column of $\mathbf{Z}_1$ (trophic variables). The correlation is 0.725. The two axes are not plotted to the same scale because they are in different units.

The first three columns of the $\mathbf{F}_1$ matrix are shown in Table 6. The first dimension has its greatest negative loadings on variables 6 (Hymenoptera) and 10 (Diptera) and its greatest positive loadings on variables 9 (Coleoptera) and 12 (Isopoda). These were also the most common prey items in the stomachs. This dimension seems to correspond roughly to a contrast between larger versus smaller prey classes. Although Diptera tend to be slightly larger than Coleoptera, they are usually softer. This contrast also corresponds to the differences in the diet of the two species when in sympatry (*P. hoffmani* consuming more Hymenoptera and Diptera, and *P. cinereus* consuming more Coleoptera and Isopoda; Adams, 1999). The other dimensions are more difficult to interpret (e.g., the second dimension is largely a contrast between Coleopter and Diptera versus larvae and Isopoda).

The $\mathbf{F}_2$ matrix is not shown because there is little interest in how each partial warp contributes to each dimension (see Rohlf, 1998). What is of interest is the implied shape change. To help interpret the meaning of the dimensions, one can estimate the shapes corresponding to the extreme values of the $\mathbf{Z}_2$ scores. The coordinates of a landmark configurations can be computed as $\hat{\mathbf{X}} = \mathbf{X}_c + \hat{\mathbf{Z}}\mathbf{P}^t$, where $\hat{\mathbf{Z}}$ is a vector of the $\mathbf{Z}_2$ scores to be visualized (see Rohlf, 1999). The thin-plate spline can be used to transform $\mathbf{X}_c$ into $\hat{\mathbf{X}}$. For one-dimensional data, the results can be displayed as a pair of shapes representing the extremes of the observed variation.

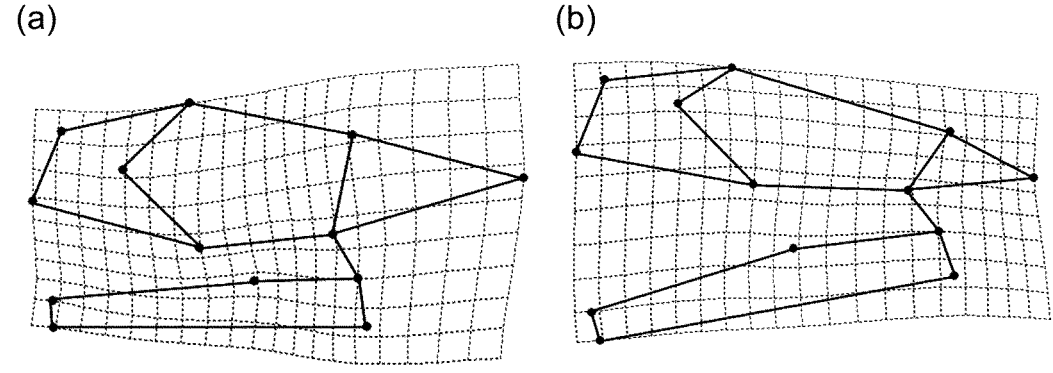

FIGURE 4. Visualization of the results of a 2B-PLS analysis estimating the shapes corresponding to a point at the negative (a) and positive (b) extremes observed for the first $\mathbf{Z}_2$ variable. Shape differences are expressed as deformations of the average shape by using thin-plate splines. Landmarks are connected with line segments to facilitate visualization (see Fig. 1 for their locations on a *Plethodon* skull).

Figure 4A shows a shape corresponding to $\hat{\mathbf{Z}} = (-0.13, 0, \ldots, 0)$ and Figure 4B shows a shape corresponding to $\hat{\mathbf{Z}} = (0.08, 0, \ldots, 0)$. As illustrated, the shape differences related to diet appear to be mostly in the length of the dentary relative to the length of the squamosal (a smaller ratio in Fig. 4A and a larger ratio in Fig. 4B). Adams (1999) discusses these results and presents a biomechanical model to explain why this type of shape difference should be related to prey size.

We also performed simulations to demonstrate that 2B-PLS analysis is able to uncover known relationships between a set of variables and partial warp scores—except for the problem of rotation when more than a single dimension is important. For example, one simulation used two normally distributed factors (independent, with $\sigma_1 = 0.01$ and $\sigma_2 = 0.008$); four variables were constructed with the scores for variables 1 and 2 being 0.9 times the first factor and the scores for variables 3 and 4 being 0.7 times the second factor. Shapes with five landmarks were constructed with scores for partial warp x_2 equal to the first factor and partial warp y_1 equal to the second factor. Independent bivariate normally distributed digitizing error ($\sigma = 0.001$) was added to each landmark. The variation among 100 superimposed specimens is shown in Figure 5. In the 2B-PLS analysis the variables were standardized but the partial warps were not.

As expected, the first two dimensions accounted for almost all of the covariance. The cumulative percentages of the squared singular values (of a total squared covariance of 0.0001280) and their percentages from the permutation test were 74.39% (68.7%), 99.95% (0.1%), 99.98% (3.1%), and the last, of course, 100%. The correlations between the sets and their percentages from the randomization test are 0.743 (0.1%), 0.699 (0.1%), 0.238 (15.3%), and 0.207 (2.3%). These results are consistent with the underlying two-factor model.

However, the $\mathbf{F}_1$ and $\mathbf{F}_2$ matrices in Table 7 do not match the known underlying factors. The first column of $\mathbf{F}_1$ is approximately a contrast between the first and last two variables and the second column of $\mathbf{F}_1$ is the sum of all four variables. Similarly, the first column of

TABLE 7. Results of a simulation, showing the first two columns of $\mathbf{F}_1$ and $\mathbf{F}_2$, singular values, and correlations.

		Dimensions	
Matrix	Variable	1	2
$\mathbf{F}_1$	1	0.533	0.379
	2	0.583	0.478
	3	−0.480	0.547
	4	−0.381	0.573
$\mathbf{F}_2$	X_1	−0.012	−0.005
	Y_1	−0.610	0.792
	X_2	0.792	0.610
	Y_2	0.006	0.013
	X_{Uni}	0.007	0.004
	Y_{Uni}	−0.010	0.001
Singular value		0.00975	0.005732
Correlation		0.743	0.699

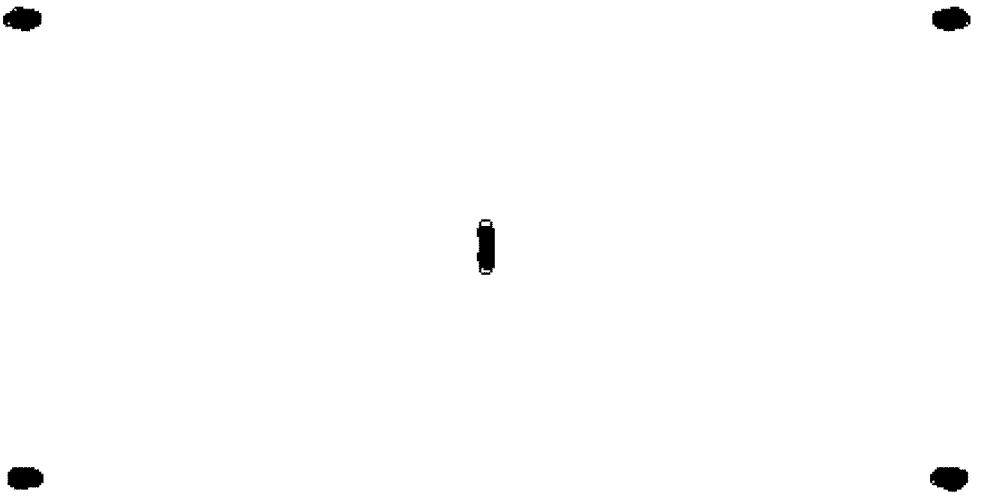

FIGURE 5. GLS superimposition showing the variation in shape of the 100 specimens used in the simulation described in the text.

$\mathbf{F}_2$ is approximately a contrast between partial warps Y_1 and X_2 and the second column of $\mathbf{F}_2$ is the sum of partial warps Y_1 and X_2. Figure 6 shows a pair of biplots. At the left is a plot of column two against column one for the $\mathbf{F}_1$ matrix superimposed on a plot of column two against column one for the $\mathbf{Z}_1$ matrix. At the right is a similar plot for the $\mathbf{Z}_2$ and $\mathbf{F}_2$ matrices. A simultaneous rotation of the axes in the two ordinations by about 53° would yield the desired alignment with the two underlying factors. That is, the first two variables and partial warp x_2 would load on one axis and the last two variables and partial warp y_1 would load on the other axis. Of course, in an actual application, we would not know that the axes should be rotated by a particular angle. Just as in a principal components analysis, we can hope that a space of the proper dimensionality will be recovered but we cannot expect the axes to necessarily line up with whatever underlying factors are responsible for the variation. Perhaps adding additional information about the specimens or some form of factor analysis will help the investigator decide which directions in the paired biplots yield the most useful interpretation.

GENERALIZATION TO COVARIATION BETWEEN TWO SHAPES

It is clear that one can easily extend the procedure described above to have matrices of both sets of variables, $\mathbf{Y}_1$ and $\mathbf{Y}_2$, correspond to shape variables. Bookstein (1997) used this technique (which he called singular warp analysis) to explore the covariation between shapes of two sets of landmarks in adjacent midsagittal longitudinal slices from magnetic resonance images of the human brain and also to study the same landmarks in adjacent midsagittal longitudinal slices. The approach is quite general. For example, this approach could be used to study the covariation between the shape of some structure in the larval stage and the shape of some other structure in adults of the same individuals. The configurations of landmarks need only be paired in some way, such as two different parts of the same individual, mating pairs, or parasite and host.

For illustration, we recorded two-dimensional coordinates of landmarks from dorsal and ventral views of the house mice skulls. The data were from a larger study by Corti and Rohlf (in prep.). Ten landmarks were recorded from the dorsal view of the skull and 14 from the ventral view for the 75 mice for which both sets of landmarks were available. The landmarks used were a subset of those in the original study. The mice were of both sexes and from four localities (representing different chromosomal races). We wanted to see what covariation there was between the relative positions of landmarks in dorsal and ventral views of a skull. As discussed above, the shape variables could

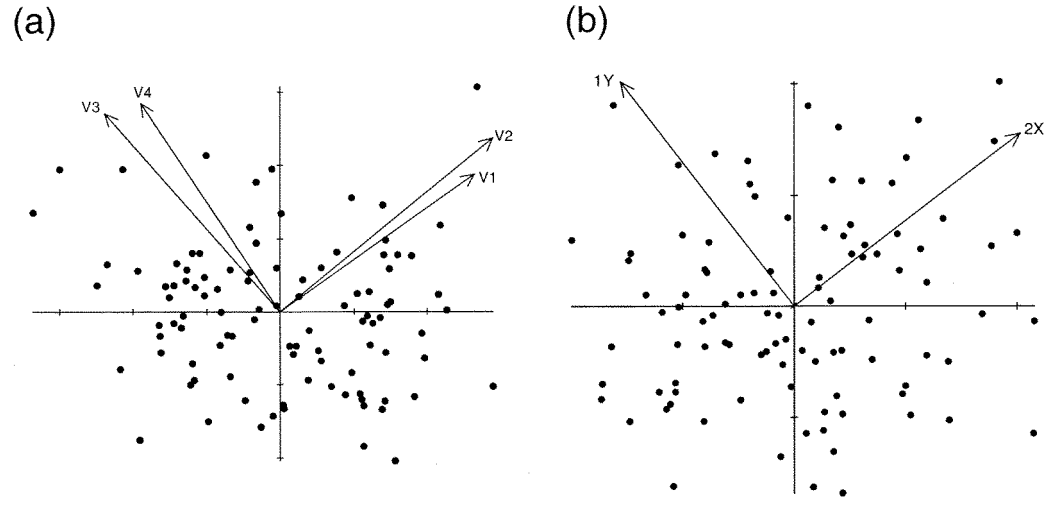

FIGURE 6. Results of a 2B-PLS analysis of simulated data. Ordinations of the 100 simulated data points are shown as biplots. The points correspond to the simulated specimens, and the vectors represent the variables as linear combinations of the axes. (a) Plot of the first two linear combinations of variables. (b) Plot of the first two linear combinations of the partial warps. The vectors corresponding to partial warps x_1 and y_2 and the two uniform components are at the origin and are indistinguishable.

be either aligned coordinates or partial warp scores. In either case, the shape variables do not need to be standardized because they are already in the same units. Thus, the $\mathbf{R}_{12}$ matrix will contain the covariances between the two sets of shape variables. Partial warp scores were computed (uniform component included) separately for the dorsal and ventral views (Fig. 7).

Table 8 shows the singular values, cumulative squared singular values (as proportions of the total, 1.0595×10^{-7}), and cross-set correlations for the first five dimensions. The results of permutation tests (using 999 random permutations) are also shown. Again, the results are largely one-dimensional. The first pair of latent variables accounts for ~84% of the squared covariance and none of the random permutations resulted in such a large percentage for the first dimension. The other singular values were much smaller and not statistically significant. All of the cumulative proportions of covariance explained are significant, but that is because the first pair of variables accounts for so much of the covariance. The correlation for the first pair of variables is 0.702 (Fig. 8 shows the corresponding scatterplot). Again, none of the random permutations achieved such a large value. The other correlations were less and of little interest (even though many were statistically significant) because the corresponding latent variables explained so little of the cross-set covariance.

TABLE 8. Results of permutation tests for the dorsal/ventral comparison for the house mouse skull data. Only the results for the first five dimensions are shown. λ_i is the ith singular value, $\sum \lambda_i^2$ is the cumulative sum of squared singular values, and r_i is the correlation for the ith pair of latent variables. Probabilities are based on the observed values plus 999 random permutations of the association between the dorsal and ventral landmarks.

Dimensions	λ_i	P	$\sum \lambda_i^2$	P	r_i	P
1	0.000298	0.001	0.837	0.001	0.702	0.001
2	0.000094	0.998	0.920	0.001	0.587	0.003
3	0.000053	1.000	0.947	0.001	0.459	0.129
4	0.000044	1.000	0.965	0.001	0.528	0.007
5	0.000042	0.998	0.982	0.001	0.519	0.002

Figure 9 shows ordinations of the 75 specimens for the first pairs of dorsal and for the ventral latent variables. Because the first latent variable explains so much of the covariation, we are most interested in the distribution along the abscissa in the plots. Figure 10 gives visualizations of the shapes corresponding to the positive ends of the first axis for the dorsal and the ventral data (locations of the landmarks on the skulls are also shown). These specimens have a narrow zygomatic bar at the squamosus. Interestingly,

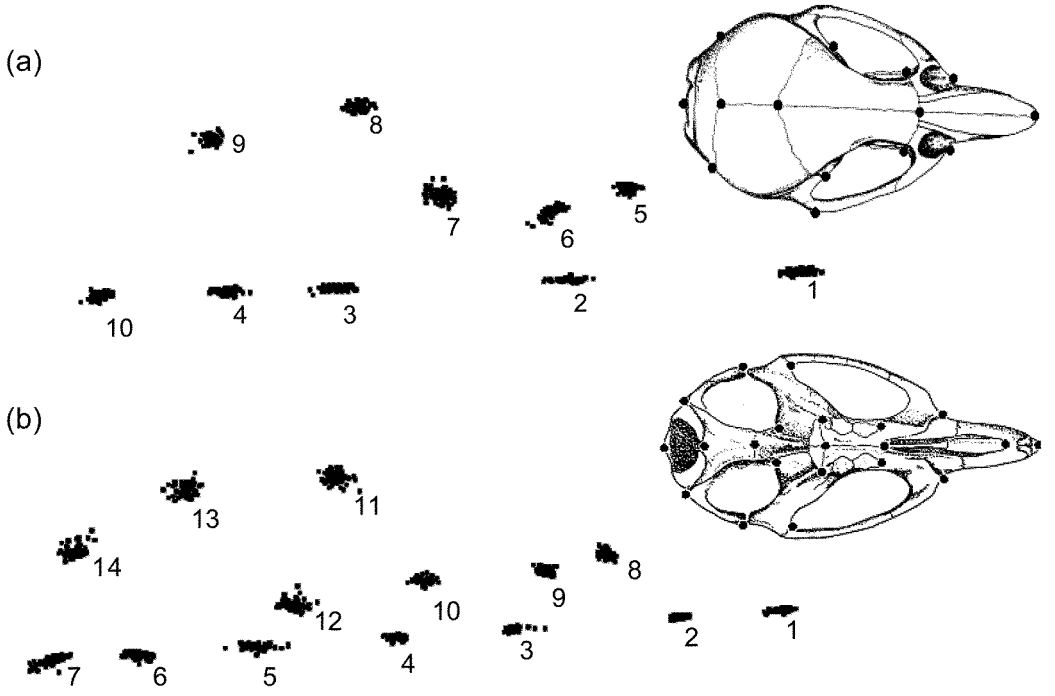

FIGURE 7. GLS superimposition for 75 house mice, *Mus musculus domesticus*. (a) Dorsal view with 10 landmarks. (b) Ventral view with 14 landmarks. Diagrams show locations of the landmarks on the skulls.

the apparent contrasting effect at the rostrum between the dorsal (landmarks 1, 2, 5, 6, 7) and the ventral (landmarks 1, 2, 3, 8, 9, 10) sides suggests a different evolution in shape in these two components. In the dorsal side, there is a long frontal bone (landmarks 2 and 3), and the origin of the zygomatic bar at the jugal (landmarks 5 and 6) is shifted backwards and inwards. In the ventral side, the molar toothrow (landmarks 9 and 10) and the fossa palatina (landmarks 2 and 3) are long, but the former is directed outwards and the latter backwards.

DISCUSSION

Although the 2B-PLS method is related to multivariate regression analysis, the kinds of applications are quite distinct. Regression is used when one wishes to see how a set of dependent variables (which could be shape variables) vary as a function of one or more independent variables. In a 2B-PLS analysis (as in CCA), the two sets of variables are treated symmetrically in an attempt to find relationships between them without assuming that one is the cause of the variation in the other. 2B-PLS is often used in an exploratory fashion to determine what combinations of variables in the two sets account most for whatever covariation there is between the two sets of variables. It can also be used in a confirmatory manner by seeing whether the linear combinations match expectations (see Sampson et al., 1989).

The 2B-PLS method differs from CCA by being used to find latent variables that can account for the covariance between the two sets of variables. CCA is used to seek pairs of linear combinations that are highly correlated, but the pairs detected need not account for much of the covariance between the two sets of variables. For that reason, CCA should be used in conjunction with redundancy analysis to make sure that the latent variables account for an appreciable proportion of the covariance (see Jackson, 1991). The 2B-PLS method is a simple direct method to obtain variables that account for as much as possible of the covariation between two sets of variables. Although the variables obtained from a 2B-PLS analysis are not expected to be as highly correlated as those obtained from a CCA, the correlations also are usually not much lower than the latter.

A limitation of the 2B-PLS method is that there is no direct test of significance, but permutation tests seem quite satisfactory. The

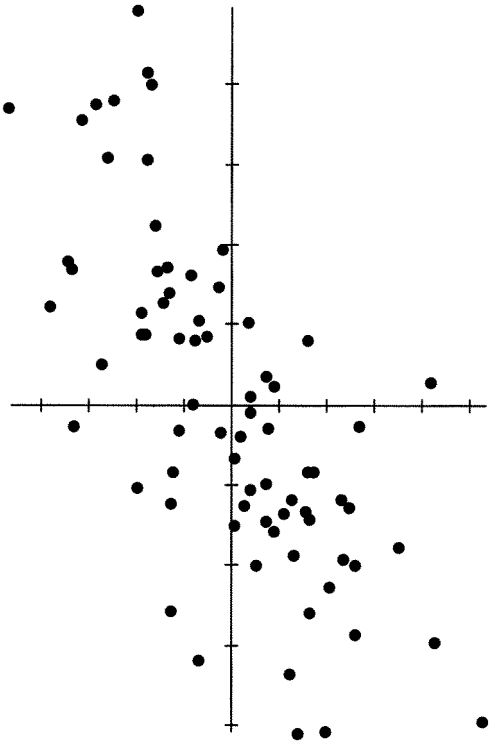

FIGURE 8. Plot of first 2B-PLS dimension for the house mouse data. Ordinate, dorsal; abscissa, ventral. Correlation is 0.702.

use of the method assumes that the variables have linear relationships with the underlying factors. Strong nonlinear relationships may lead to misleading results. For example, a single underlying factor with highly nonlinear effects will probably result in two or more

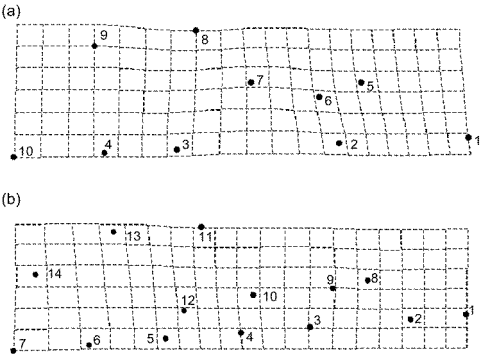

FIGURE 10. Thin-plate spline visualization of shapes of skulls of the house mouse as a deformation of the average shape. The shapes correspond to the positive end of the abscissa in the plots in Figure 9. (a) Dorsal landmarks. (b) Ventral landmarks.

significant dimensions. This problem should usually be detectable from an examination of the ordinations and from plots of the variables against the latent variables. One solution is to transform the variables and then repeat the analysis. Another approach is to include additional variables to account for the nonlinear relationships, as was done in Rohlf (1970). Alternatively one can use monotone nonlinear scalings of the variables optimized for prediction by the variables in the other set (Sampson et al., 1989).

The analysis has a wide range of potential applications in systematics. The *Plethodon* example from Adams (1999) represents a very successful application. This method was also used by Corti et al. (1996) to study covariation between three-dimensional landmarks

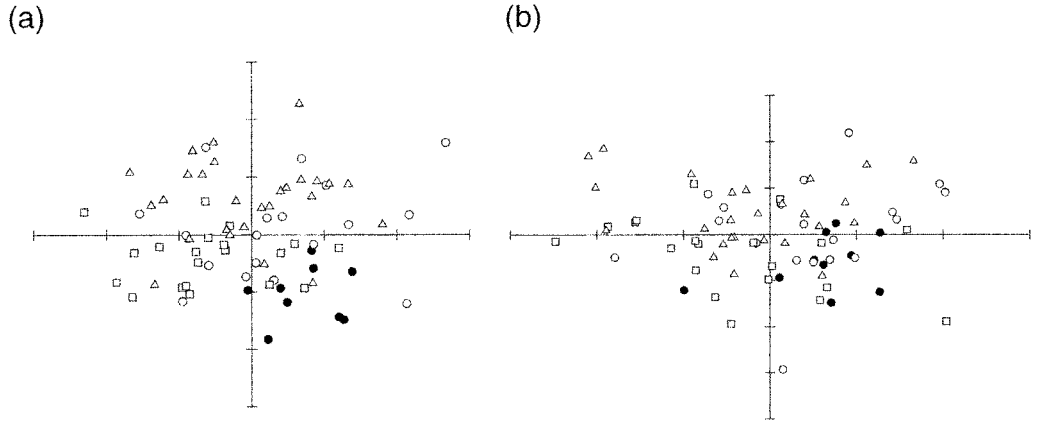

FIGURE 9. Ordinations based on the first two 2B-PLS dimensions for chromosomal races in the house mouse (Corti and Rohlf, in prep.). (a) Ordination using dorsal landmarks. (b) Ordination using ventral landmarks. ○ = Upper Valtellina ($2n = 24$); ● = Burano ($2n = 40$); △ = Orobian ($2n = 22$); ❒ = Poschiavo ($2n = 26$).

of the mandible of the mole rat *Spalax ehrenbergi* and a set of ecogeographic variables (including temperature, humidity, rainfall, soil type, and vegetation). Similarly, Fadda and Corti (1998) studied geographic variation in three-dimensional landmarks of the skull of the African Rodent *Arvicanthis* in the Nile Valley, using variables of temperature and rainfall during various periods of the year. They were able to demonstrate consistent scenarios of morphometric variation across the different environments represented by those variables, interpreted as adaptations, however, they used the correlations rather than the covariances we advocate here.

Another potential use is in studies in which separate analyses have been performed on different two-dimensional views of a three-dimensional structure (e.g., the dorsal and ventral sides of the skull; Corti and Fadda, 1996; Corti and Rohlf, in prep.). The relationship between patterns found in separate views needs to be explored to understand better the shape variation in three dimensions. In the case of Corti and Fadda (1996), distance matrices were correlated. Although this may allow establishing some agreement between patterns of variation drawn from the separate analyses, it does not show the amount and kind of covariation of the different two-dimensional views. The use of 2B-PLS analysis showed that mice vary differently in the dorsal and ventral side, mostly in the region of the rostrum and palate. This is important in interpreting directions in phenotypic evolution, because different rates or directions in shape change can affect different parts or substructures of the skull, resulting in different functionality.

tpsPLS software implements the application of 2B-PLS to the analysis of shape variation. This program is freely available from the Stony Brook morphometrics web site at http://life.bio.sunysb.edu/morph. A PLS module for the analysis of paired sets of variables in available as part of the NTSYSpc program for multivariate data analysis (Rohlf, 1997).

ACKNOWLEDGMENTS

The helpful comments by Fred Bookstein and an anonymous reviewer are greatly appreciated. This work was supported in part by a grant from the Ecological and Evolutionary Physiology (IBN-9728160) program of the National Science Foundation. Work on this paper was begun while F.J.R. was a Visiting Professor at the University of Rome, "La Sapienza". This article is contribution no. 1055 from the Graduate Studies in Ecology and Evolution, State University of New York at Stony Brook.

REFERENCES

ADAMS, D. C. 1999. Ecological character displacement in *Plethodon* and methods for shape analysis of articulated structures. Ph.D. Thesis. State Univ. New York at Stony Brook.

BOOKSTEIN, F. L. 1982. The geometric meaning of soft modeling, with some generalizations. Pages 55–74 *in* Systems under indirect observation: causality-structure-prediction. (K. G. Jöreskog and H. Wold, eds.). North Holland Publishing Company, New York.

BOOKSTEIN, F. L. 1986. The elements of latent variable models. Adv. Dev. Psychol. 4:203–230.

BOOKSTEIN, F. L. 1989. Principal warps: thin-plate splines and the decomposition of deformations. IEEE Trans. Pattern Anal. Mach. Intell. 11:567–585.

BOOKSTEIN, F. L. 1991. Morphometric tools for landmark data: geometry and biology. Cambridge Univ. Press, New York.

BOOKSTEIN, F. L. 1996. A standard formula for the uniform shape component in landmark data. *In* Advances in morphometrics (L. F. Marcus, M. Corti, A. Loy, G. J. P. Naylor, and D. E. Slice, eds.). NATO ASI Ser. 284:153–168.

BOOKSTEIN, F. L. 1997. Analyzing shape data from multiple sources: the role of the bending energy matrix. Pages 106–115 *in* Proceedings in the art and science of Bayesian image analysis (K. V. Mardia, C. A. Gill, and I. L. Dryden, eds.). Leeds University Press, Leeds, England.

BOOKSTEIN, F. L., A. STREISSGUTH, P. SAMPSON, AND H. BARR. 1996. Exploiting redundant measurement of dose and behavioral outcome: new methods from the teratology of alcohol. Dev. Psychol. 32:404–415.

CORTI, M., AND C. FADDA. 1996. Systematics of *Arvicanthis* (Rodentia, Muridae) from the Horn of Africa: a geometric morphometrics evaluation. Ital. J. Zool. 63:185–192.

CORTI, M., C. FADDA, S. SIMSON, AND E. NEVO. 1996. Size and shape variation in the mandible of the fossorial rodent *Spalax ehrenbergi*. *In* Advances in morphometrics (L. F. Marcus, M. Corti, A. Loy, G. J. P. Naylor, and D. E. Slice, eds.). NATO ASI Ser. 284:303–320.

DRYDEN, I. L., AND K. V. MARDIA. 1998. Statistical shape analysis. John Wiley & Sons, New York.

DUNN, L. C. 1922. The effect of inbreeding on the bones of the fowl., Pages 1–112 *in* Bulletin 152. Storrs Agricultural Experiment Station, Storrs, Connecticut.

ECKART, C., AND G. YOUNG. 1936. The approximation of one matrix by another of lower rank. Psychometrika 1:211–218.

FADDA, C., AND M. CORTI. 1998. Geographic variation of *Arvicanthis* (Rodentia, Muridae) in the Nile Valley. Z. Säugetierk. 63:104–113.

JACKSON, J. E. 1991. A user's guide to principal components. John Wiley & Sons, New York.

JÖRESKOG, K. G., AND H. WOLD. 1982. Systems under indirect observation: causality–structure–prediction. Parts I and II. Elsevier, North Holland, Amsterdam.

KENT, J. T. 1994. The complex Bingham distribution and shape analysis. J. R. Stat. Soc. B 56:285–299.

MANLY, B. F. J. 1994. Multivariate statistical methods: a primer, 2nd edition. Chapman & Hall, New York.

MARCUS, L. F. 1990. Traditional morphometrics. Pages 77–122 *in* Proceedings of the Michigan morphometrics workshop, volume 2 (F. J. Rohlf and F. L. Bookstein, eds.). Univ. Michigan Museum of Zoology, Ann Arbor, Michigan.

MARCUS, L. F., M. CORTI, A. LOY, G. J. P. NAYLOR, AND D. E. SLICE (eds.). 1996. Advances in morphometrics, NATO ASI Ser. 284:1–587.

MCINTOSH, A. R., F. BOOKSTEIN, J. HAXBY, AND C. GRADY. 1996. Multivariate analysis of functional brain images using partial least squares. NeuroImage 3:143–157.

ROHLF, F. J. 1970. Adaptive hierarchical clustering schemes. Syst. Zool. 19:58-82.

ROHLF, F. J. 1993. Relative warp analysis and an example of its application to mosquito wings. Pages 131–159 *in* Contributions to morphometrics (L. F. Marcus, E. Bello, and A. Garcia-Valdecasas, eds.). Museo Nacional de Ciencias Naturales, Madrid.

ROHLF, F. J. 1996. Morphometric spaces, shape components and the effects of linear transformations. *In* Advances in morphometrics (L. F. Marcus, M. Corti, A. Loy, G. J. P. Naylor, and D. E. Slice, eds.). NATO ASI Ser. 284:117–129.

ROHLF, F. J. 1997. NTSYS-pc: Numerical taxonomy and multivariate analysis system. Exeter Software, Setauket, New York.

ROHLF, F. J. 1998. On applications of geometric morphometrics to studies of ontogeny and phylogeny. Syst. Biol. 47:147–158.

ROHLF, F. J. 1999. Shape statistics: Procrustes superimpositions and tangent spaces. J. Classif., 16:197–223.

ROHLF, F. J., AND L. F. MARCUS. 1993. A revolution in morphometrics. Trends Ecol. Evol. 8:129–132.

ROHLF, F. J., AND D. E. SLICE. 1990. Extensions of the Procrustes method for the optimal superimposition of landmarks. Syst. Zool. 39:40–59.

SAMPSON, P. D., A. P. STREISSGUTH, H. M. BARR, AND F. L. BOOKSTEIN. 1989. Neurobehavioral effects of prenatal alcohol: part II. partial least squares analysis. Neurotoxicol. Teratol. 11:477–491.

SMALL, C. G. 1996. The statistical theory of shape. Springer, New York.

STREISSGUTH, A. P., F. L. BOOKSTEIN, P. D. SAMPSON, AND H. M. BARR. 1993. The enduring effects of prenatal alcohol exposure on child development: birth through seven years, a partial least squares solution. Univ. Michigan Press, Ann Arbor, Michigan.

Received 12 February 1999; accepted 3 May 1999
Associate Editor: R. Olmstead